Electric Starter-Generator for More-Electric Aircraft

by

Gabriel Borge Martínez

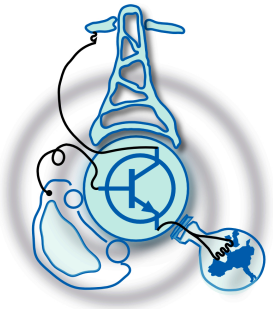

Submitted to the Department of Electrical Engineering, Electronics, Computers and Systems)
in partial fulfillment of the requirements for the degree of
Master degree in Electrical Energy Conversion and Power Systems
at the
UNIVERSIDAD DE OVIEDO
July 2016

© Universidad de Oviedo 2016. All rights reserved.

Author .....

Certified by .....
Pablo García Fernández
Dr. Associate Professor
Thesis Supervisor

Certified by .....
Serhiy Bozhko
Dr. Associate Professor
Thesis Supervisor

Electric Starter-Generator for More-Electric Aircraft

by

Gabriel Borge Martínez

Submitted to the Department of Electrical Engineering, Electronics, Computers and Systems)
on July 22, 2016, in partial fulfillment of the
requirements for the degree of
Master degree in Electrical Energy Conversion and Power Systems

Abstract

The present work aims the development of the control system for starter-generator system for future More-Electric Aircraft (MEA) platforms. The system will combine functions of engine electric start with electrical power generation to supply on-board loads. The system should provide electric power quality according to aerospace standards independently on engine operation mode.

For the design and control, the following steps have been carried out:

I Brief summary of the principle of a Surface Permanent Magnets Synchronous Machine (SPMSM) (including simulation parameters) and background screening of MEA.

II Study of *abc* to *dq* transformation system and stationary to synchronous reference frame transformation have been explained to simplify the control.

III Introduction to AC brushless equations: in phase coordinates and in U*dq* coordinates.

IV From the previous equations, Laplace transform and Taylor's theorem have been included for the analysis of small signal.

V Simulation processes through linear equations to develop the current loop

VI Simulation processes through linear equations to develop the torque/speed loop

VII Simulation outcomes using PSIM software.

VIII Conclusions

The following abbreviations and symbols will be used along the document:

Abbreviations and symbols.	
V_{abc}	Stator voltages in phase coordinates.
i_{abc}	Stator currents in phase coordinates.
λ_{abc}	Stator flux in phase coordinates.
v_{qs},v_{ds}	Stator q and d axes voltages.
i_{qs},i_{ds}	Stator q and d axes currents.
λ_{qs},λ_{ds}	Stator q and d axes flux linkages.
λ_{PM}	Permanent magnet flux linkage.
L_q,L_d	Stator q and d axes inductances.
R_s	Stator resistance.
p	Derivative operator.
w_e,θ_e	Electrical angular speed and position.
w_r,θ_r	Rotor angular speed and position.
T_e	Torque of the machine.
T_L	Torque of the load.
Superscripts.	
r,e	Rotor or synchronous reference frame.
s	Stator or stationary reference frame.
$*$	Reference signal.
Subscripts.	
0	Initial state

Thesis Supervisor: Pablo García Fernández
Title: Dr. Associate Professor

Thesis Supervisor: Serhiy Bozhko
Title: Dr. Associate Professor

Acknowledgments

I would like to acknowledge Erasmus+ program to part-finance this work at the University of Nottingham (UK). In addition, I would like to thanks *Dr. Serhiy Bozhko* and *Dr. Seang Shen Yeoh* for supervising my work and showing me new concepts to apply in the field of controlling aircraft motors.

I should therefore like to thank all people that has supported me during this Master specially *Dr. Pablo García Fernández* as tutor of my work.

I would also like to thank *my family* and my girlfriend *Natalia Gómez* for their ongoing support. Thank you everyone,

Gabriel Borge

Contents

List of Figures

List of Tables

Chapter 1

Thesis Introduction

1.1 Introduction

This project is based on the understanding of the operational background of SPMSM. The SPMSM has many advantages over Induction Machines (IM). The most relevant is the high efficiency coming from the fact that magnetising current is not a part of the stator current. In IM the reactive current is carried by the stator winding for the rotor excitation while in SPMSM the flux is created by the magnet material in the rotor. Self excitation brings about various benefits, such as the elimination of the rotor copper losses. For this report, a simulation of SPMSM will be carried out with the following parameters (Table 1.1).

Table 1.1: Machine details.

SPMSM parameters	
Stator resistance $R_s(m\Omega)$	1.058
Stator d inductance $L_d(\mu H)$	99
Stator q inductance $L_q(\mu H)$	99
Number of poles P	6
Magnet flux-linkage $\lambda_{PM}(V \cdot s)$	0.03644
Inertia $J(kg \cdot m^2)$	0.403
Friction $F(N \cdot m \cdot s)$	0.001
Rated power $P_{rated}(kW)$	45

1.1.1 Project Background

The More-Electric Aircraft (MEA) is one of the main trends in a modern aircraft engineering aiming to boost the performance and reliability of tomorrow's aircraft. Like any vehicle, an aircraft needs an auxiliary power in the same way a car needs a battery to power its windshield wipers, dome-line or electric windows.

Four types of energy are used to power systems on todays aircraft: mechanical, hydraulic, pneumatic and electrical. They provide the power needed for flight control to manage energy production by engines and generators, to manage aircrat configuration like the actuation of landing gear and brakes,for passanger comfort and services, and for air conditioning and pressurization. In turn, it results in significant increase in on-board electric power demand. Hence the role of electric power generation system is of great importance. Existing solutions has severe limitations to meet requirements of future more-electric aircraft therefore new topologies should be considered.

The project will investigate a potential solution based on permanent-magnet machine controlled by active front-end power electronic converter. This system topology will conveniently manage reversing of power flow direction; hence will be able of performing both starting and generating functions. The project will focus on control design procedure for this system. The main design criteria should be developed in order to meet electrical power quality according to standard MIL-STD-704, and the system design should demonstrate significant improvement in performance compare to existing solutions.

1.1.2 Methodology

Through this project a small-signal mathematical model of the SPMSM based starter-generator system will be developed. It means that a control structure will be designed to provide the engine starting. At the next stage, the control system will be expanded to provide the generation mode, including particularities of operation in flux-weakening mode. Stability of the designed system in a presence of non-linear loads will be also assessed by linearization using small-signal analysis. The design

will be confirmed by numerical simulations using linearized and non-linear models with PSIM software.

1.2 Objectives

The project will aim for development of control system for starter-generator system for future more-electric aircraft platforms. The system will combine functions of engine electric start with electrical power generation to supply on-board loads. The system should provide electric power quality according to aerospace standards independently on engine operation mode.

In order to carry out the proposed study, the following objectives are stablish:

- General reading and familiarisation with MEA principles in the project context.
- Familiarisation with MATLAB/Simulink/SimPower and embedded linear systems analysis tools.
- Refreshing control system design principles and methods applicable to the project (timing as above as well).
- General study into the starter-generator systems, literature review, and understanding the topology of the system to be developed and clarification of design approach.
- Design of starter mode controls, including development of MATLAB models using UNOTT in-house software libraries.
- Design of generation mode controls, including flux-weakening and DC voltage controls, including MATLAB model development.
- Simulation of the system performance under different scenario in motoring and generating modes and verification of design.
- Summarizing results and making conclusions.

1.3 Opportunities

In traditional aircraft, multiple systems may use one type or a combination of types of energy, including electrical, hydraulic, mechanical, and pneumatic energy. However, all energy types have different drawbacks, including the sacrifice of total engine efficiency in the process of harvesting a particular energy, as with hydraulic and pneumatic systems. The goal for future aircraft is to replace most of the major systems currently utilizing nonelectric power, such as environmental controls and engine start, with new electrical systems to improve a variety of aircraft characteristics, such as efficiency, emissions, reliability, and maintenance costs.

Aircraft system configuration and comparison between tranditional and More Electric Aircraft are shown in Fig. 1-1 and Table 1.2.

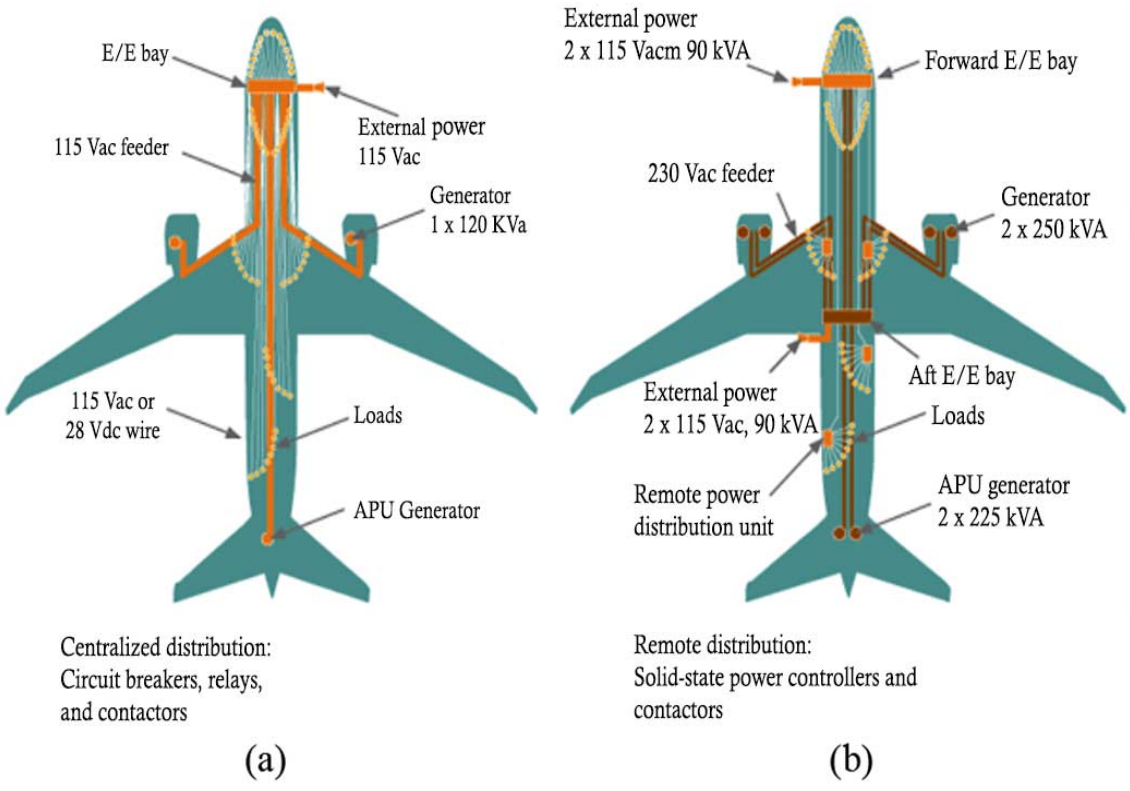

Figure 1-1: Comparison between traditional (b) and MEA (a).

Table 1.2: Traditional vs MEA.

	Traditional	**More Electric Aircraft**
Power system distribution	Centralised power system distribution. The power is generated on the wings near the main engines and in the aft.	Remote distribution and simplify network: • Increase efficiency. • Decrease losses between generation and consumption.
Control system distribution	Mechanical Constant Frequency Generation: • Mechanical gearbox creates a constant speed shaft from a variable speed input. • Constant speed shaft drives the Generator: – Voltage control used for the generator. – 400Hz voltage supply fixed frequency • Expensive to purchase and maintain: – Single source due to patents.	Variable Frequency Generation: • Generator provides variable frequency supply: – Voltage control around generator • Direct connection between generator and power bus: – Simple and reliable generation • Nearly all aircraft loads will require power converters for control:
Enviromental control system	Bleed air architecture for temperature and pressure regulation	Electric power regulate the temperature and pressure. Pneumatic system and air ducts are removed.
Electrification of hydraulic system	Hydraulic systems are used in aircraft for primary and secondary surface control, braking, landing gear, and many other important functions. These hydraulic systems are dependent on mechanically driven actuators.	Electro-hydraulic actuators (EHAs) or electromechanical actuators (EMAs). EHAs are considered advantageous because of weight, volume, dispatch reliability, and cost advantages.

1.4 Thesis structure

The Thesis document will gather to the maximum extent possible the carried out study covering all the accomplished stages to fulfil the proposed objectives in section 1.2. The Thesis document is organized as follows, matching with the followed methodology.

- *Chapter 1* presents the thesis introduction including the project background and methodology. Objectives, opportunities and this section.
- *Chapter 2* describe the transformation method.
- *Chapter 3* shows the main equations to use in this master thesis.
- *Chapter 4* describes the Taylor method to use in the equations of the previous chapter.
- *Chapter 5*, a simulation with linear equations has been developed including the initial design for the PI regulators in the current and speed loops.
- *Chapter 6* a simulation with linear equations has been developed including the final design for the PI regulators in the current and speed loops.
- *Chapter 7* flux weakening include the novelty of the work to shows the hight speed control.
- *Chapter 8* conclude with the specific and general conclusions and future prospect for this technology.

Chapter 2

Transformations

2.0.1 *abc* to *dq* transformation

For the simulation of this machine, the d and q axis position must be considered. The equation 2.1 is used to convert abc system to dq system. Fig. 2-1 shown the system.

$$f_{dq} = \frac{2}{3} \cdot \left(f_a + f_b \cdot e^{-j\frac{2\pi}{3}} + f_c \cdot e^{j\frac{2\pi}{3}} \right) \tag{2.1}$$

Where expressing Euler's formula:

$$e^{-j\frac{2\pi}{3}} = \cos\left(-\frac{2\pi}{3}\right) - j \cdot \sin\left(-\frac{2\pi}{3}\right) \tag{2.2}$$

$$e^{j\frac{2\pi}{3}} = \cos\left(\frac{2\pi}{3}\right) - j \cdot \sin\left(\frac{2\pi}{3}\right) \tag{2.3}$$

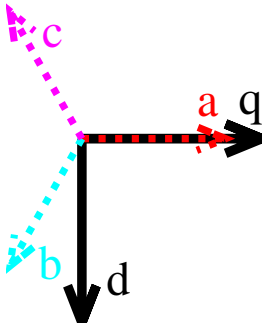

Figure 2-1: The dq system use.

2.0.2 Stationary to synchronous reference frame transformation

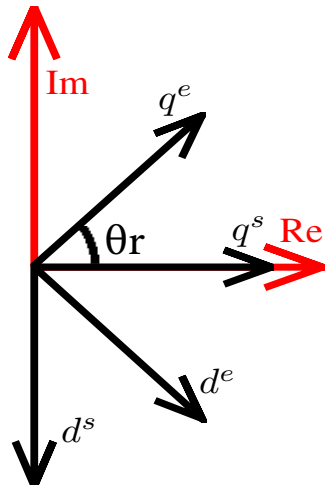

Figure 2-2: Transformation reference frame.

Fig. 2-2 shows both system of reference: stationary reference frame (f^s_{dq}) and synchronous reference frame (f^e_{dq}), being f any variable to transform. In the Fig. 2-2 imaginary and real axis can be also seen and the rotation (θ_r) between both system of reference can be represented with Euler formula (equation 2.4).

$$e^{-j\cdot\theta_r} = \cos\theta_r - j\cdot\sin\theta_r \tag{2.4}$$

For doing the transformation of the stationary reference frame to synchronous reference frame is only necessary multiply by the rotation (equation 2.5). Final result is shown in matricial form in equation 2.8. T in equation 2.9 is the rotation matrix.

$$f^e_{dq} = e^{-j\cdot\theta_r}\cdot f^s_{dq} \tag{2.5}$$

$$f^e_q - j\cdot f^e_d \;=\; (\cos\theta_r - j\cdot\sin\theta_r)\cdot\left(f^s_q - j\cdot f^s_d\right) \tag{2.6}$$

$$f_q^e - j \cdot f_d^e \;=\; \left(f_q^s \cdot \cos\theta_r - f_d^s \cdot \sin\theta_r\right) - \; j \cdot \left(f_q^s \cdot \sin\theta_r + f_d^s \cdot \cos\theta_r\right) \tag{2.7}$$

$$\begin{bmatrix} f_q^e \\ f_d^e \end{bmatrix} = \begin{bmatrix} \cos\theta_r & -\sin\theta_r \\ \sin\theta_r & \cos\theta_r \end{bmatrix} \cdot \begin{bmatrix} f_q^s \\ f_d^s \end{bmatrix} \tag{2.8}$$

$$f_{dq}^e = T \cdot f_{dq}^s \tag{2.9}$$

Chapter 3

Motor equations [4]

3.0.1 AC brushless equations in phase coordinates

The voltage equation of the stator circuits is developed in equation 3.1, where R and L are characteristics of the machine. The flux linkage is expressed in equation 3.2. Moreover, the torque is expressed in equations 3.3 and 3.4, while the mechanical to the electrical speed is given by equation 3.5.

$$V_{abc} = R \cdot i_{abc} + \frac{d}{dt}\lambda_{abc} \tag{3.1}$$

$$\lambda_{abc} = \lambda_{PM} + L \cdot i_{abc} \tag{3.2}$$

$$T_e = P \cdot \frac{\partial \lambda_{abc}}{\partial \theta_e} \cdot i_{abc}^T \tag{3.3}$$

$$T_e - T_L = J \cdot \frac{dw_r}{dt} \tag{3.4}$$

$$w_e = \frac{P}{2} \cdot w_r \xRightarrow{\int} \theta_e = \frac{P}{2} \cdot \theta_r \tag{3.5}$$

3.0.2 Equations of AC brushless equations in dq coordinates

The complex vector expressions are obtained from above equations (3.1, 3.2, 3.3 and 3.4) using the expressions defined in section $II.A$. The result for each equation is the following (expressed in matrix form):

$$\begin{bmatrix} v_{qs}^r \\ v_{ds}^r \end{bmatrix} = \begin{bmatrix} R_s & 0 \\ 0 & R_s \end{bmatrix} \cdot \begin{bmatrix} i_{qs}^r \\ i_{ds}^r \end{bmatrix} + \begin{bmatrix} p & w_r \\ -w_r & p \end{bmatrix} \cdot \begin{bmatrix} \lambda_{qs}^r \\ \lambda_{ds}^r \end{bmatrix} \tag{3.6}$$

The previous equations 3.6 show the voltage in the stator viewed in the rotor reference frame. In the same way the flux linkage equation is given by equation 3.7.

$$\begin{bmatrix} \lambda_{qs}^r \\ \lambda_{ds}^r \end{bmatrix} = \begin{bmatrix} L_q & 0 \\ 0 & L_d \end{bmatrix} \cdot \begin{bmatrix} i_{qs}^r \\ i_{ds}^r \end{bmatrix} + \overbrace{\begin{bmatrix} w_r \cdot \lambda_{PM} \\ 0 \end{bmatrix}}^{BEMF} \tag{3.7}$$

As can be seen in equation 3.7, the last term represents the Back Electro-Motive Force (BEMF). This is proportional to the rotor speed. Combining both equations 3.6 and 3.7, the following equation is obtained (equation 3.8):

$$\begin{bmatrix} v_{qs}^r \\ v_{ds}^r \end{bmatrix} = \begin{bmatrix} R_s & 0 \\ 0 & R_s \end{bmatrix} \cdot \begin{bmatrix} i_{qs}^r \\ i_{ds}^r \end{bmatrix} + \begin{bmatrix} p & w_r \\ -w_r & p \end{bmatrix} \cdot \begin{bmatrix} L_q & 0 \\ 0 & L_d \end{bmatrix} \cdot \begin{bmatrix} i_{qs}^r \\ i_{ds}^r \end{bmatrix} + \begin{bmatrix} w_r \cdot \lambda_{PM} \\ 0 \end{bmatrix} \tag{3.8}$$

The last equations define the torque system (equations 3.9 and 3.10). Following the same procedure than before:

$$T_e = \frac{3}{2} \cdot \frac{P}{2} \left[\underbrace{\lambda_{PM} \cdot i_{qs}^r}_{Magnetic-Torque} + \underbrace{(L_d - L_q)\, i_{qs}^r \cdot i_{ds}^r}_{Reluctance-Torque} \right] \tag{3.9}$$

$$T_e - T_L = J \cdot \frac{dw_r}{dt} \tag{3.10}$$

All the equations are referred to the rotor reference frame. Those equations will be transformed using Laplace transform and Taylor's theorem to performed the small signal analysis. furthermore, they will be also used for the non-linear simulation.

Chapter 4

Small signal analysis

4.0.1 Equations of AC brushless equations in phase coordinates

In this section, using Laplace transform and Taylor's theorem (equation 4.1) non-linear functions can be approximated in reduced environment around a point $x\epsilon(a,b)$ by a polynomial which coefficients depend on the derivatives function at that point.

$$f(x) = f(a) + \frac{f'(a)}{1!} \cdot (x - a) \tag{4.1}$$

By using the Taylor's theorem and Laplace transform in equations 3.8, 3.9 and 3.10, the corresponding equations are for voltages and torque:

$$\Delta v_{ds}^r = (R_s + L_d \cdot s) \cdot \Delta i_{ds}^r - \underbrace{L_q \cdot i_{qs0}^r \cdot \Delta w_e - L_q \cdot w_{e0} \cdot \Delta i_{qs}^r}_{feedforward\ term} \tag{4.2}$$

$$\Delta v_{qs}^r = (R_s + L_q \cdot s) \cdot \Delta i_{qs}^r + \underbrace{L_d \cdot i_{ds0}^r \cdot \Delta w_e + L_d \cdot w_{e0} \cdot \Delta i_{ds}^r + \lambda_{PM} \cdot \Delta w_e}_{feedforward\ term} \tag{4.3}$$

$$\Delta T_e = \frac{3}{2} \cdot \frac{P}{2} \cdot [\lambda_{PM} \cdot \Delta i^r_{qs} + (L_d - L_q) \cdot \left(i^r_{ds0} \cdot \Delta i^r_{qs} + i^r_{qs0} \cdot \Delta i^r_{ds}\right)] \quad (4.4)$$

$$\Delta T_e - \Delta T_L = J \cdot \frac{2}{P} \cdot s \cdot \Delta w_e \quad (4.5)$$

Chapter 5

Initial design

5.1 Simulation with Linear equations

5.1.1 Current loop

To perform the current regulation, the stator voltage equations have to be taken into account (the induced voltages equations are (5.1) and (5.2)):

$$v_{qs}^r = R_s i_{qs}^r + L_q \frac{di_{qs}^r}{dt} + \lambda_{qs}^r \quad (5.1)$$

$$v_{ds}^r = R_s i_{ds}^r + L_d \frac{di_{ds}^r}{dt} + \lambda_{ds}^r \quad (5.2)$$

Therefore, the transfer functions can be represented as follows:

$$\frac{v_{qs}^r - \lambda_{qs}^r}{i_{qs}^r} = \frac{1}{L_q s + R_s} \quad (5.3)$$

$$\frac{v_{ds}^r - \lambda_{ds}^r}{i_{ds}^r} = \frac{1}{L_d s + R_s} \quad (5.4)$$

The previous outcome implies that PI regulators should be used for the current regulation. A closed loop bandwidth of 1000 Hz ($BW_i[Hz]$) is used. Then, the regulators and their parameters are [2]:

$$\frac{\left(v_{qs}^{r}-\lambda_{qs}^{r}\right)^{*}}{i_{qs}^{r*}-i_{qs}^{r}} = K_{iq}\left(1+\frac{1}{Ti_{iq}\cdot s}\right) \tag{5.5}$$

$$K_{iq} = 2\pi\cdot BW_{i}[Hz]\cdot L_{q} = 0.622 \tag{5.6}$$

$$Ti_{iq} = \frac{L_{q}}{R_{s}} = 93.57\ ms \tag{5.7}$$

$$\frac{\left(v_{ds}^{r}-\lambda_{ds}^{r}\right)^{*}}{i_{ds}^{r*}-i_{ds}^{r}} = K_{id}\left(1+\frac{1}{Ti_{id}\cdot s}\right) \tag{5.8}$$

$$K_{id} = 2\pi\cdot BW_{i}[Hz]\cdot L_{d} = 0.622 \tag{5.9}$$

$$Ti_{id} = \frac{L_{d}}{R_{s}} = 93.57\ ms \tag{5.10}$$

The induced voltages (λ_{ds}^{r} and λ_{qs}^{r}) are not negligible, so the final control actions (v_{qs}^{r*} and v_{ds}^{r*}) can be obtained by summing the regulator control actions and the estimated induced voltages as seen in the following equations (the estimated induced voltages can be calculated with (3.7) using the measured speed):

$$v_{qs}^{r*} = \left(v_{qs}^{r}-\lambda_{qs}^{r}\right)^{*}+\widehat{\lambda_{qs}^{r}} \tag{5.11}$$

$$v_{ds}^{r*} = \left(v_{ds}^{r}-\lambda_{ds}^{r}\right)^{*}+\widehat{\lambda_{ds}^{r}} \tag{5.12}$$

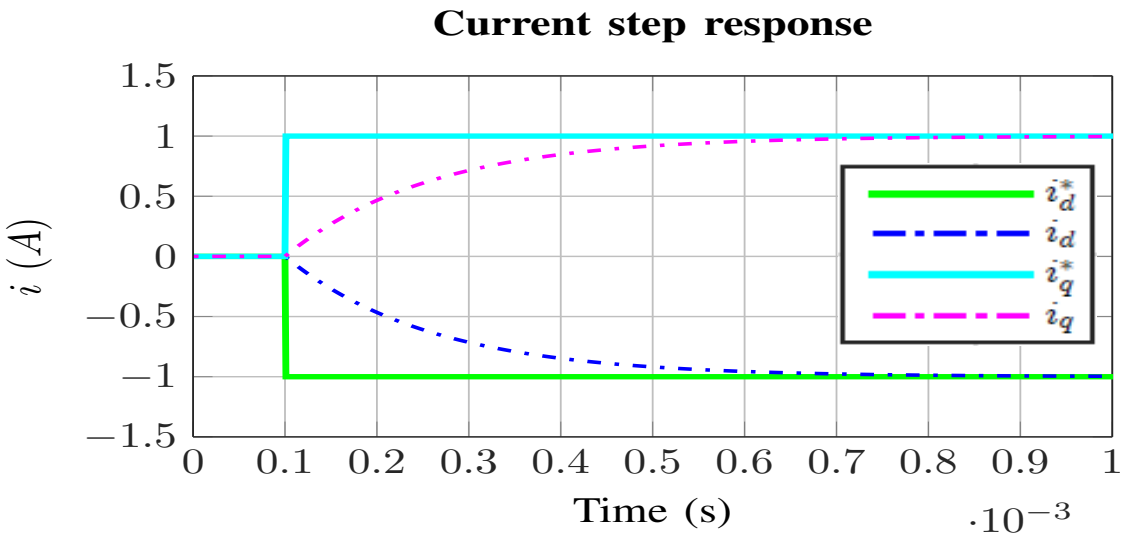

Figure 5-1: Detail of results of current regulation.

As can be seen in Fig. 5-1, the settling time (time at which the actual values are the 95% of the steady state values) of the currents is approximately 0.58 ms (0.1 ms after the step change of the current references). Therefore, the effective bandwidth of the current regulation is [2]:

$$\tau_i = \frac{t_s}{3} = \frac{0.48\ ms}{3} = 0.16\ ms \tag{5.13}$$

$$BW_i[rad/s] = \frac{1}{\tau_i} = 6250\ rad/s \tag{5.14}$$

$$BW_i[Hz] = \frac{BW_i[rad/s]}{2\pi} = 994.71\ Hz \simeq 1000\ Hz \tag{5.15}$$

5.1.2 Speed loop

To perform the speed regulation, the torque/speed equation has to be taken into account:

$$T - T_L = J\frac{d\omega_r}{dt} + B\omega_r \tag{5.16}$$

Therefore, the transfer function can be represented as follows:

$$\frac{T_e - T_L}{\omega_r} = \frac{1}{Js + B} \tag{5.17}$$

This implies that PI regulator should be used for the speed regulation. A closed loop bandwidth of 25 Hz ($BW_\omega[Hz]$) will be used. Then, the regulator and its parameters are [2]:

$$\frac{(T_e - T_L)^*}{\omega_r^* - \omega_r} = K_\omega \left(1 + \frac{1}{Ti_\omega \cdot s}\right) \tag{5.18}$$

$$K_\omega = 2\pi \cdot BW_\omega[Hz] \cdot J = 63.3 \tag{5.19}$$

$$Ti_\omega = \frac{J}{B} = \tau_{mech} = 403\ s \tag{5.20}$$

In a similar way that in (5.11) and (5.12), the final control action (T^*) can be obtained by summing the regulator control action and the estimated load torque. However, although it is possible to calculate a estimation of the load torque in this case, the parameters which determines that torque can vary or can be difficult to determine. Therefore, the estimated load torque will be neglected and the final control action will be equal to the regulator control action:

$$T^* = (T_e - T_L)^* \tag{5.21}$$

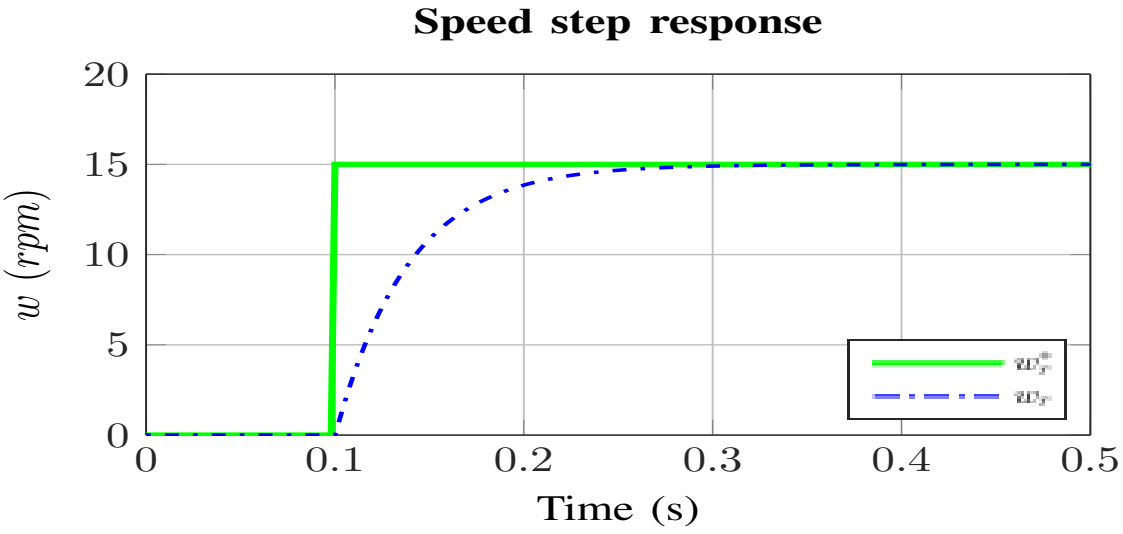

Figure 5-2: Results of speed regulation to step changes.

Taking into account all the calculations seen before, it is possible to perform a simulation that computes the behavior of the speed regulation when the required speed changes. For this simulation, the load moment of inertia (J_L) is set to 0. The

results are shown in Fig. 5-2.

Apparently, the control speed loop seems to work properly (Fig. 5-2). However, if a torque load (T_L)is applied to the system the speed regulation is not working correctly because the system would need a lot of time to obtain a zero speed error (Fig. 5-3).Then, the bandwidth requirement would not be accomplished.

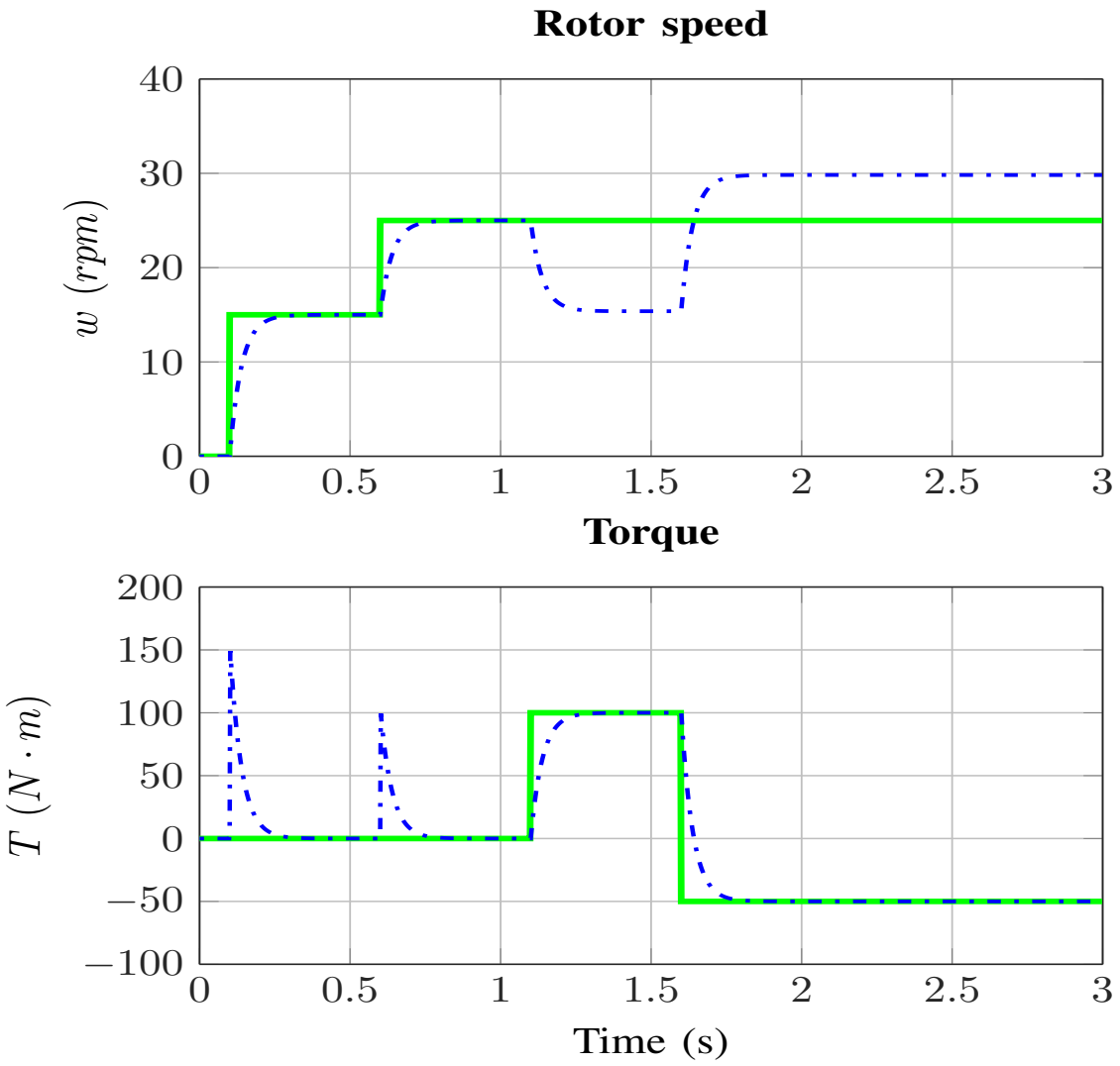

Figure 5-3: Results of speed regulation with torque load changes.

An alternative is to use the active damping. For that, a virtual damping is used to improve the system performance. To determine the active damping, it is necessary a virtual damping coefficient ($\widehat{B}$). In this case, the value of $\widehat{B}$ will be 3000 times B:

$$\widehat{B} \;=\; 3000 \cdot B = 3 \; N.m.s \tag{5.22}$$

Now, the transfer function can be represented as follows:

$$\frac{T_e - T_L}{\omega_r} \;=\; \frac{1}{Js + \left(B + \widehat{B}\right)} \tag{5.23}$$

In addition, the regulator parameters are [2]:

$$K_\omega \;=\; 2\pi \cdot BW_\omega[Hz] \cdot J = 63.3 \tag{5.24}$$

$$Ti_\omega \;=\; \frac{J}{B + \widehat{B}} = 134.29 \; ms \tag{5.25}$$

Finally, the final control action is:

$$T^* \;=\; (T_e - T_L)^* - \widehat{B}\omega_r \tag{5.26}$$

The simulation of the system with active damping are shown in Fig. 5-4.

As can be seen in Fig. 5-4, the settling time (time at which the actual value is the 95% of the steady state value) of the speed is approximately 0.389 s (379 ms after the step change of the speed reference). Therefore, the effective bandwidth of the speed regulation is [2]:

$$\tau_\omega \;=\; \frac{t_s}{3} = \frac{379 \; ms}{3} = 126.33 \; ms \tag{5.27}$$

$$BW_\omega[rad/s] \;=\; \frac{1}{\tau_\omega} = 7.92 \; rad/s \tag{5.28}$$

$$BW_\omega[Hz] \;=\; \frac{BW_\omega[rad/s]}{2\pi} = 1.26 \; Hz \tag{5.29}$$

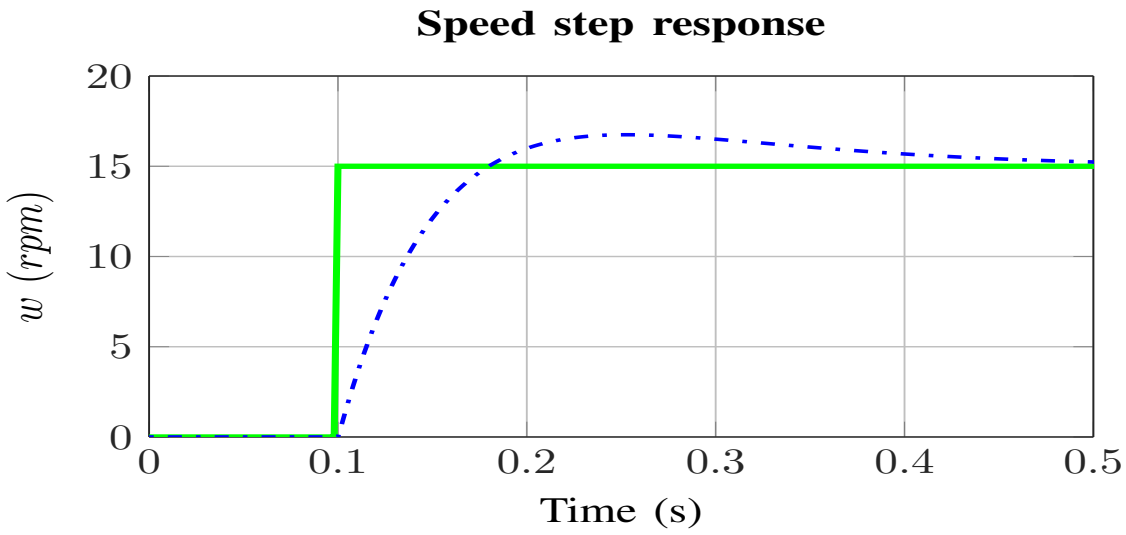

Figure 5-4: Results of speed regulation to step changes with active damping.

5.1.3 PSIM simulation

Two simulations have been performed; the first one shows the results without the active dumping in the control speed regulator and the second one with the active dumping in the regulation.

In Fig. 5-5 and Fig. 5-6 the following results were represented:

- Reference rotor speed (w_r^*) and rotor speed (w_r).
- Reference q axis current (i_q^*) and q axis current (i_q).
- Reference d axis current (i_d^*) and d axis current (i_d).
- Reference torque load (T_L) and torque in the machine (T_e).

Simulation without active dumping

In Fig. 5-5 the system performance was assessed in relation with the speed step changes in the first second. In the second second, step torque changes were evaluated. Finally, in the last second, step currents in d axes were identified.

The main outcome on the previous Fig. 5-5 is that a change in the torques provoke that the error speed is not zero value.

Simulation with active dumping

For the simulation using active damping, the previous procedure was repeated. The results can be seen in Fig. 5-6. In the first second the speed step changes vary. In the second second, step torques were identified and in the last one, step currents in d axes occurred.

The main outcome on the previous Fig. 5-6 is that a change in the torques provoke zero error speed value.

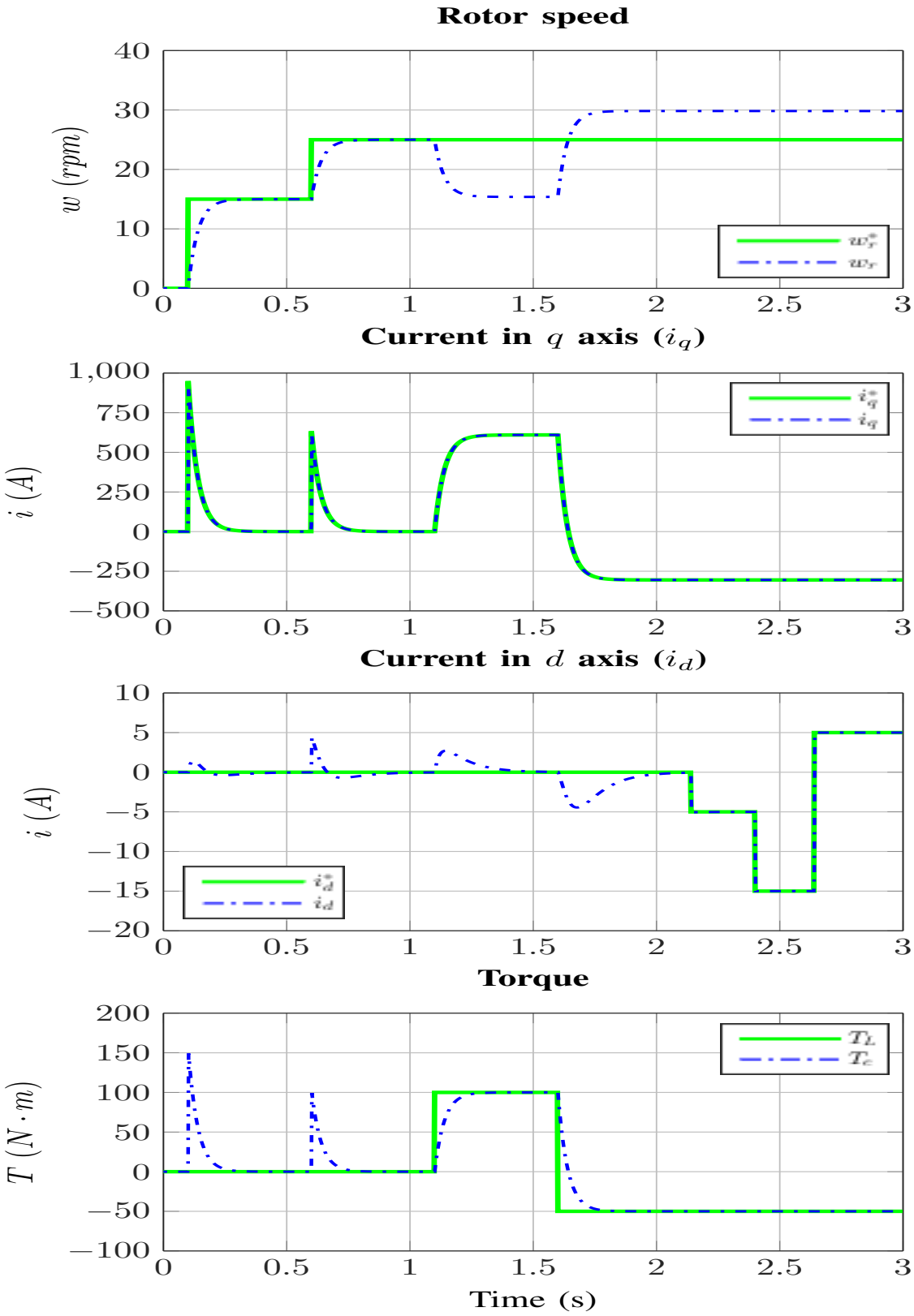

Figure 5-5: Voltages, currents and torques without active dumping.

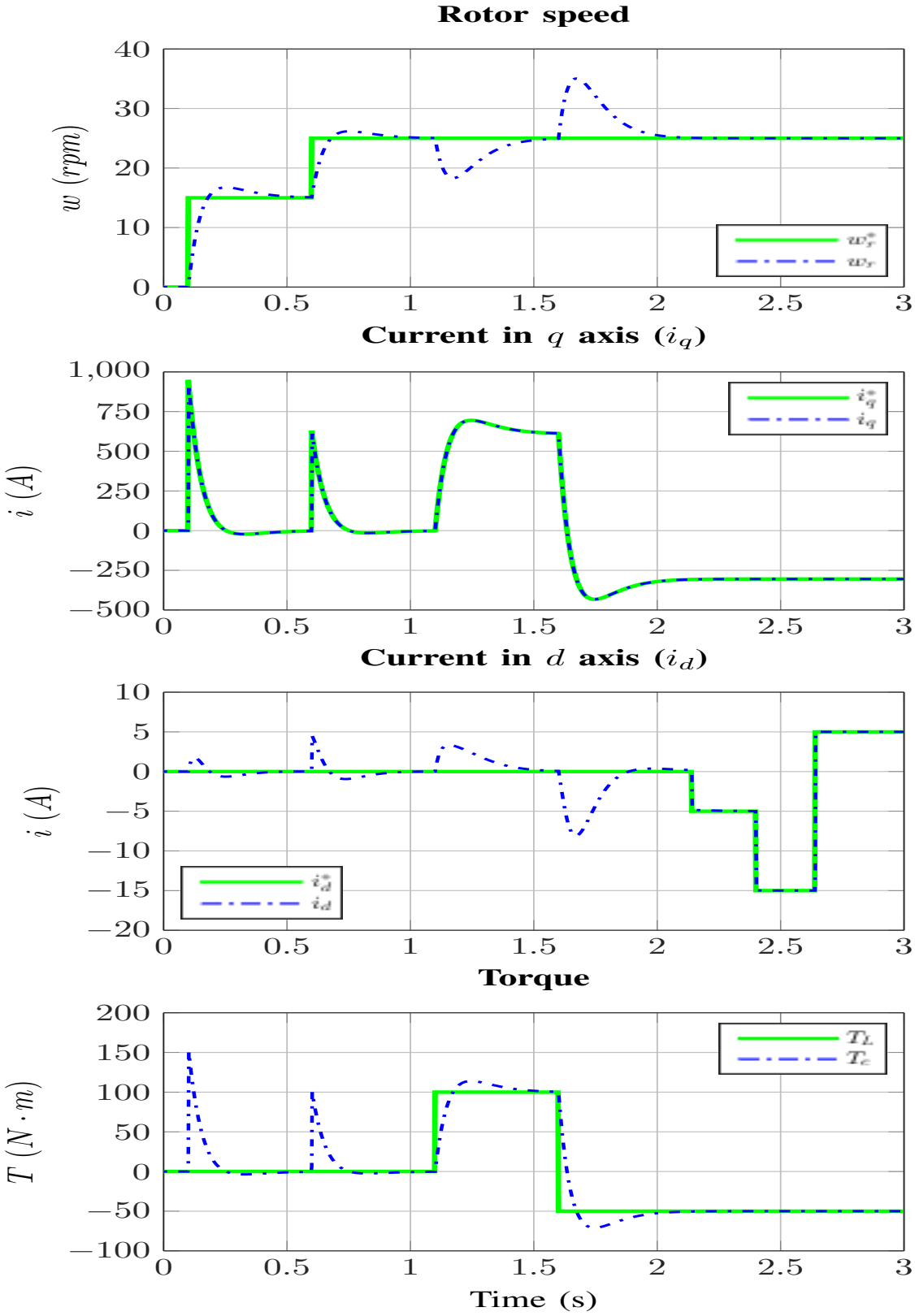

Figure 5-6: Voltages, currents and torques with active damping.

Chapter 6

Final design

Previous chapter showed the PI design using the zero pole cancellation method. Nonetheless, this method does not fulfil the current requirements for aircraft.

Then another model is proposed to overcome the last aircraft specifications

6.1 Simulation with Linear equations

6.1.1 Current loop

To perform the current regulation, the following Fig. 6-1 has been considered in order to analyse the system.

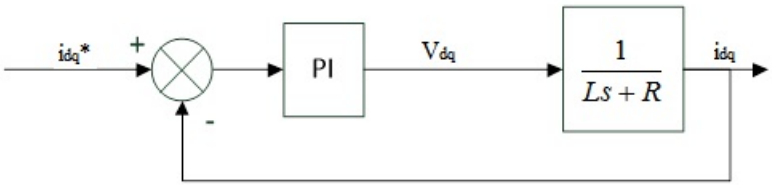

Figure 6-1: Current loop for control design.

The PI regulator transfer function is shown in equations 5.5 and 5.6. Morover, the transfer function obtained from the block diagram is the following (equation 6.1):

$$G_s = \frac{\frac{K_{p_{dq}}}{L_{dq}} \cdot s + \frac{K_{p_{dq}}}{K_{i_{dq}} \cdot L_{dq}}}{s^2 + \frac{R_s + K_{p_{dq}}}{L_{dq}} \cdot s + \frac{K_{p_{dq}}}{T_{i_{dq}} \cdot L_{dq}}} \quad (6.1)$$

$$M_s = \frac{K \cdot w_n^2}{s^2 + 2 \cdot \xi \cdot w_n \cdot s + w_n^2} \quad (6.2)$$

Doing a comparison between the transfer function above (equation 6.1) and the second order transfer function (equation 6.2). It can be seen that the denominator is very similar. This similitude is considered for the PI design.

In order to get that the current control loop work properly, $T_{i_{dq}}$ and $K_{p_{dq}}$ must be put correctly. The specifications (considering also a bandwidth of 1000 Hz ($BW_i[Hz]$)) which have been considered for the final design are:

$$w_n = 2 \cdot \pi \cdot BW_i[Hz] = 2 \cdot \pi \cdot 1000 \quad (6.3)$$

$$\xi = \frac{\sqrt{2}}{2} \quad (6.4)$$

In this case, the final value for both constants equalling the denominator terms are:

$$K_{p_{dq}} = 2 \cdot \xi \cdot w_n \cdot L_{dq} - R_s = 0.869 \quad (6.5)$$

$$T_{i_{dq}} = L_{dq} \cdot \frac{w_n^2}{K_{p_{dq}}} = 0.222\ ms \quad (6.6)$$

The induced voltages (λ_{ds}^r and λ_{qs}^r) are not negligible as in the previous chapter.

As can be seen in Fig. 6-2, the settling time (time at which the actual values are the 95% of the steady state values) of the currents is approximately 0.679 ms (0.579 ms after the step change of the current references). Therefore, the effective bandwidth of the current regulation is [2]:

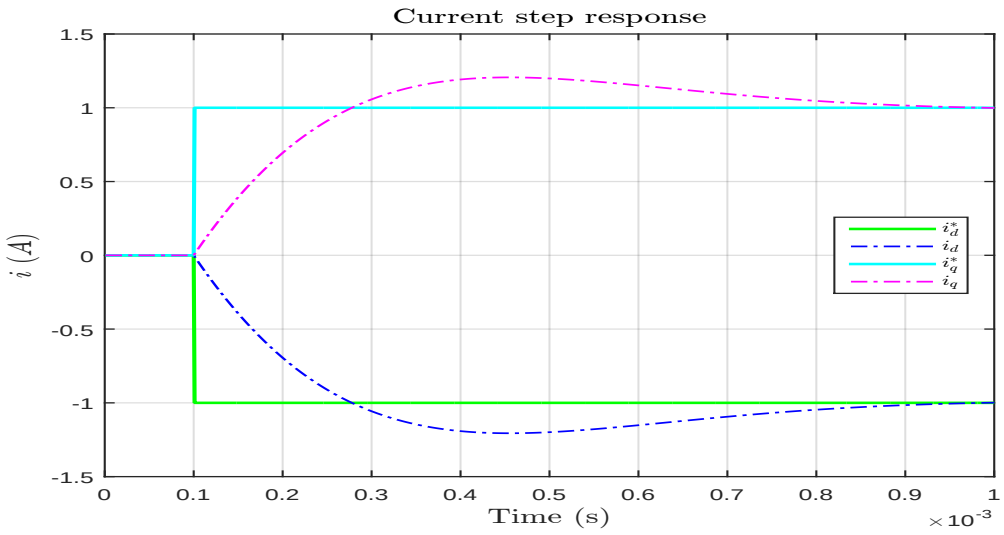

Figure 6-2: Detail of results of current regulation.

$$\tau_i = \frac{t_s}{3} = \frac{0.48\ ms}{3} = 0.193\ ms \tag{6.7}$$

$$BW_i[rad/s] = \frac{1}{\tau_i} = 5181\ rad/s \tag{6.8}$$

$$BW_i[Hz] = \frac{BW_i[rad/s]}{2\pi} = 824.58\ Hz \tag{6.9}$$

6.1.2 Speed loop

To perform the speed regulation, the torque/speed equation has to be taken into account equation 5.16. Morover, the following Fig. 6-3 has been considered in order to analyse the system.

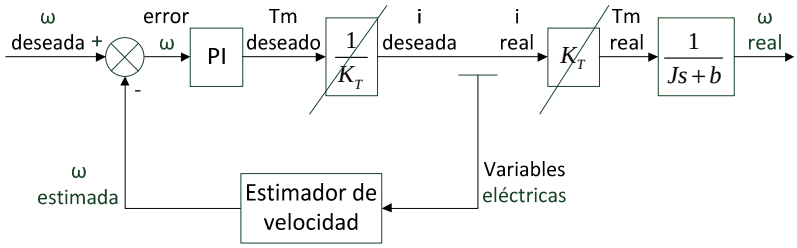

Figure 6-3: Speed loop for control design.

The PI regulator transfer function is shown in equations 5.18. Furthermore, the

transfer function obtained from the block diagram is the following (equation 6.10):

$$G_s = \frac{\frac{K_{p_\omega}}{J} \cdot s + \frac{K_{p_\omega}}{K_{i_\omega} \cdot J}}{s^2 + \frac{B+K_{p_\omega}}{J} \cdot s + \frac{K_{p_\omega}}{T_{i_\omega} \cdot J}} \tag{6.10}$$

$$M_s = \frac{K \cdot w_n^2}{s^2 + 2 \cdot \xi \cdot w_n \cdot s + w_n^2} \tag{6.11}$$

Doing a comparison between the transfer function above (equation 6.10) and the second order transfer function (equation 6.11). It can be seen that the denominator is very similar. This similitude is considered for the PI design.

In order to get that the current control loop work properly, T_{i_ω} and K_{p_ω} must be put correctly. The specifications (considering also a closed loop bandwidth of 25 Hz ($BW_\omega[Hz]$) will be used) which have been considered for the final design are:

$$w_n = 2 \cdot \pi \cdot BW_\omega[Hz] = 2 \cdot \pi \cdot 25 \tag{6.12}$$

$$\xi = \frac{\sqrt{2}}{2} \tag{6.13}$$

In this case, the final value for both constants equalling the denominator terms are:

$$K_{p_\omega} = 2 \cdot \xi \cdot w_n \cdot J - B = 89.52 \tag{6.14}$$

$$T_{i_\omega} = J \cdot \frac{w_n^2}{K_{p_\omega}} = 9 \cdot 10^{-3}\ s \tag{6.15}$$

Taking into account all the calculations seen before, it is possible to perform a simulation that computes the behaviour of the speed regulation when the required speed changes. For this simulation, the load moment of inertia (J_L) is set to 0. The results are shown in Fig. 6-4.

Comparing whit the first simulation, if a torque load (T_L) is applied to the system the speed regulation is working correctly as can be seen in Fig. 6-5).

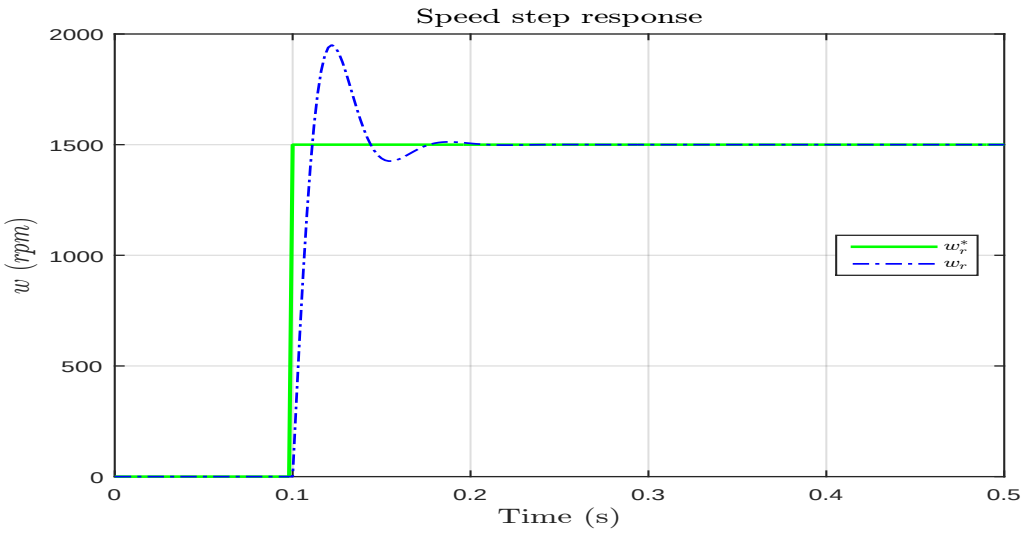

Figure 6-4: Results of speed regulation to step changes.

As can be seen in Fig. 6-4, the settling time (time at which the actual value is the 95% of the steady state value) of the speed is approximately 0.1396 s (0.0396 ms after the step change of the speed reference). Therefore, the effective bandwidth of the speed regulation is [2]:

$$\tau_\omega = \frac{t_s}{3} = \frac{39.6\ ms}{3} = 13.2\ ms \tag{6.16}$$

$$BW_\omega[rad/s] = \frac{1}{\tau_\omega} = 75.76\ rad/s \tag{6.17}$$

$$BW_\omega[Hz] = \frac{BW_\omega[rad/s]}{2\pi} = 12.06\ Hz \tag{6.18}$$

6.1.3 PSIM simulation

The same simulation which was done in the previous chapter has been performed with the actual design.

In Fig. 6-6 the following results were represented:

- Reference rotor speed (w_r^*) and rotor speed (w_r).
- Reference q axis current (i_q^*) and q axis current (i_q).

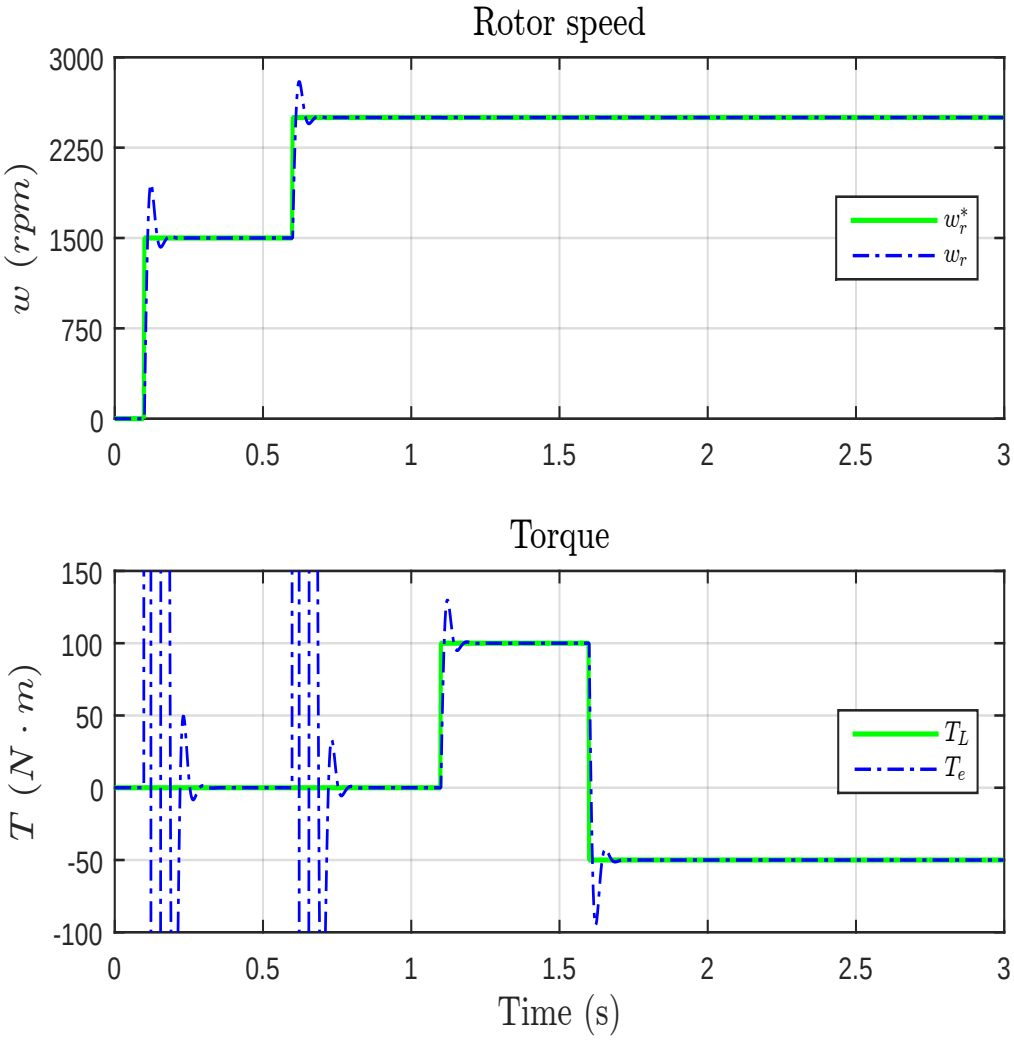

Figure 6-5: Results of speed regulation with torque load changes.

- Reference d axis current (i_d^*) and d axis current (i_d).
- Reference torque load (T_L) and torque in the machine (T_e).

Simulation without active dumping

In Fig. 6-6 the system performance was assessed in relation with the speed step changes in the first second. In the second second, step torque changes were evaluated. Finally, in the last second, step currents in d axes were identified.

The main outcome on the previous Fig. 5-5 is that a change in the torques provoke that the error speed is zero value.

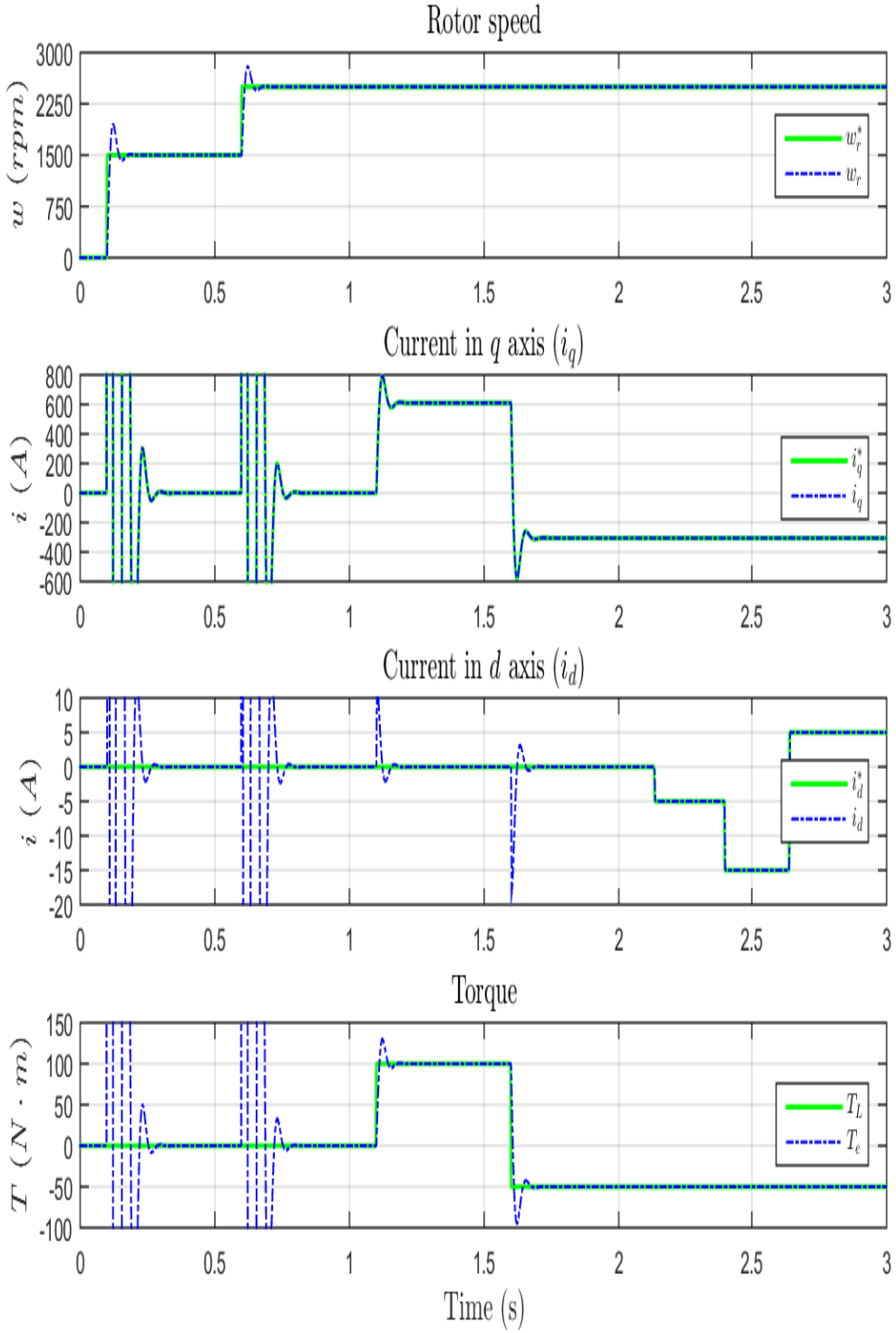

Figure 6-6: Voltages, currents and torques without active dumping.

Chapter 7

Flux weakening [6]

The flux weakening is included to increment the rotational speed of the machine.

To perform the flux weakening design it has been necessary the previous chapter of PIs design. In this chapter the loop controllers will be shown and a simulation will be done in order to understand its behaviour.

7.1 Structure of the control system

In this methodology there are to control system structure:

- Starter mode.
- Generator mode.

Each structure will be detailed in the following subsections.

Following equations 7.2 and 7.1 has been considered to implement de flux weakening control:

$$|V| = \sqrt{v_d^2 + v_q^2} \tag{7.1}$$

$$i_q = \sqrt{i_{maxima}^2 - i_d^2} \tag{7.2}$$

Starter mode

The purpose of this part is to drive the aircraft turbine using the PMM to a certain speed. An outer loop controller is used and the active power is regulated in relation to the speed demand that can be seen in Fig. 7-1

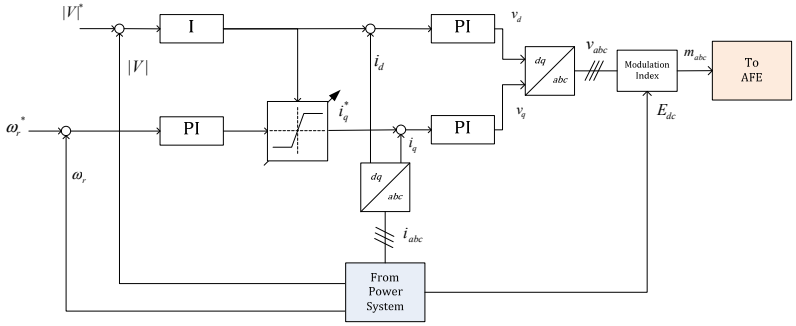

Figure 7-1: Control structure used in starter mode [6].

The field weakening control would be connected on the outer i_d loop which regulates reactive power.

Generator mode

The DC link power is regulated with regards to the connecting loads and must be controlled it voltage. The field weakening controller ensures through their connection that the voltage is worked within range for all speeds. Fig. 7-4 shows generator mode structure.

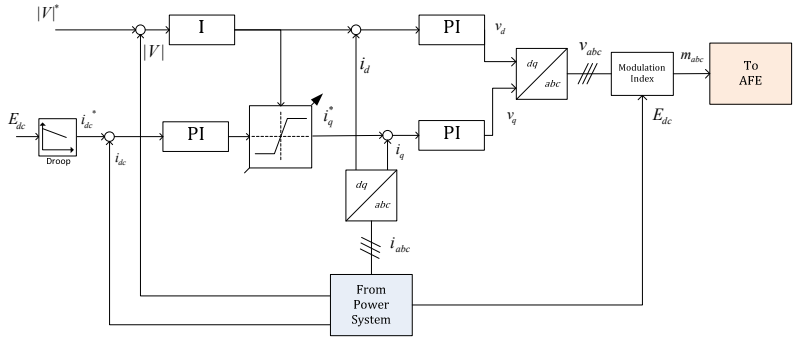

Figure 7-2: Control structure used in generator mode [6].

7.1.1 PI design

For both operation modes, there is a dynamic limiter based on equation 7.2. The use of the limiter would create 2 states: limited and not limited. These states should be taking into account during starter mode.

To get common control design for this controller, the open loop plant should be derived in:

- Starter mode with i_q not limited.
- Starter mode with i_q limited.
- Generator mode with i_q not limited.
- Generator mode with i_q limited.

Open loop plant: Starter mode with i_q not limited

Following Fig. 7-3 shows the block diagram in starter mode when i_q is not limited:

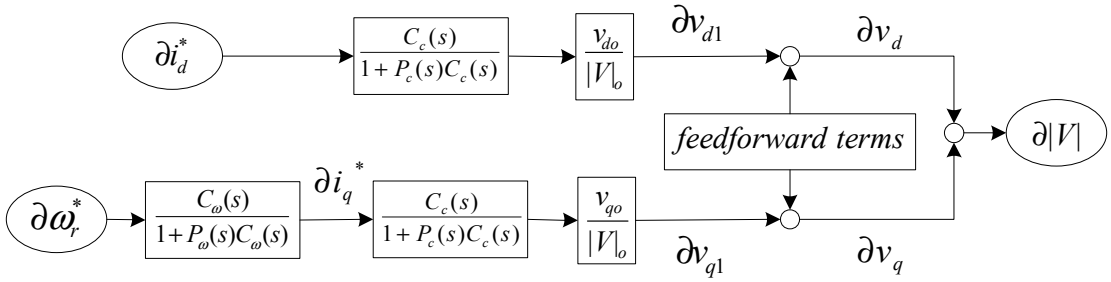

Figure 7-3: Linearized block diagram in starter mode when i_q is not limited [6].

From above Fig. 7-3, can be obtained the transfer function: $\frac{|V|}{i_d^*}$ (Fig. 7.3). Require equations 4.2 and 4.3.

$$\frac{V}{i_d^*} = \frac{(2\xi w_n L - R)s + w_n^2 L}{L(s^2 + 2\xi w_n s + w_n^2)} \left[\frac{v_{d0}}{V_0}(R + Ls) + \frac{v_{q0}}{V_0} L w_{e0}\right] \tag{7.3}$$

In order to see that the transfer function is right a simulation has been performance. This simulations consist of compare a step in open loop in the transfer

function $\frac{|V|}{i_d^*}$ whit a step provoke in the system in the simulation.

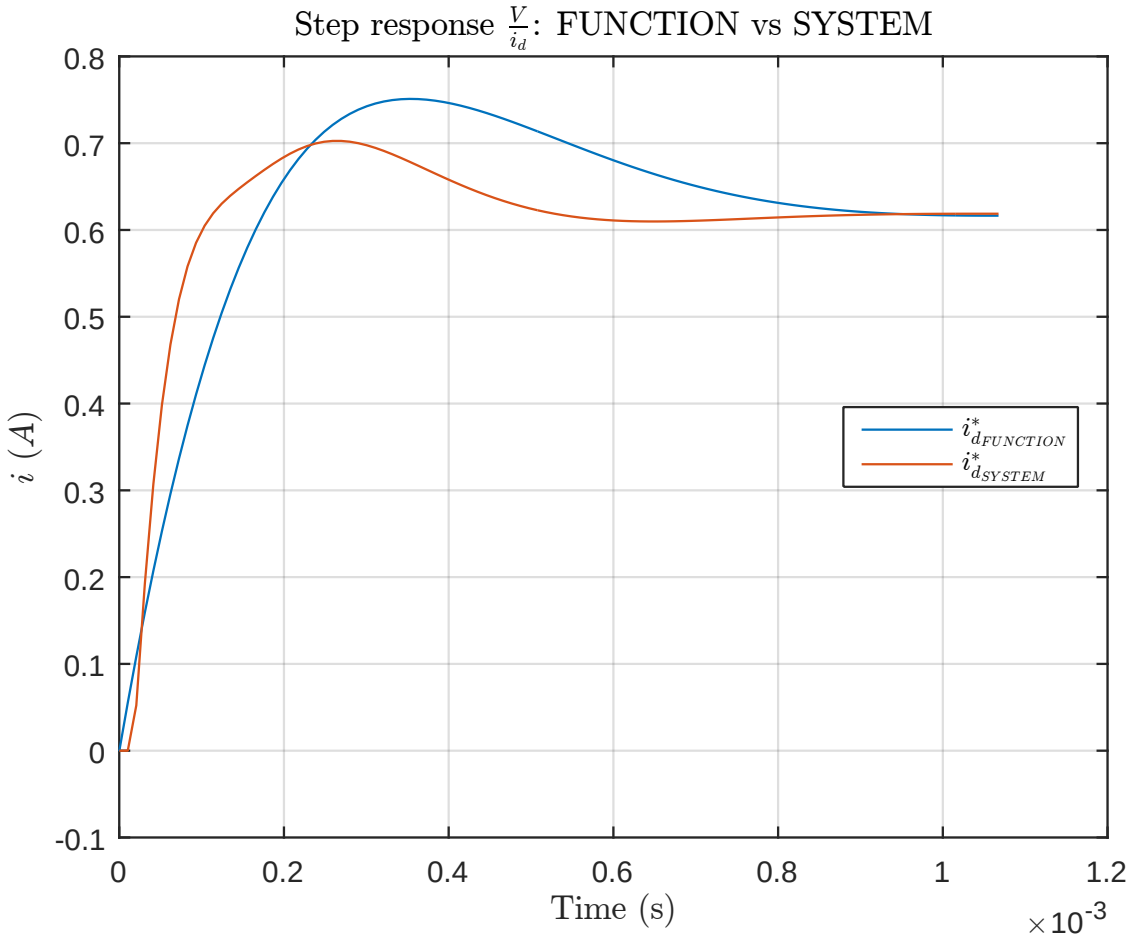

Figure 7-4: Simulation to check the function transfer in comparison with the system in the simulation.

7.1.2 Future prospect

Future prospect should be the following items. The analysis procedure should be the same that in the previous case.

- Starter mode with i_q limited.
- Generator mode with i_q not limited.
- Generator mode with i_q limited.

7.1.3 PSIM simulation

Fig. 7-5 show the simulation results of the flux weakening for the rotor speed,magnitude voltage, i_q torque current, i_d flux weakening current and torque versus time.

As can be seen, from the rotor speed graph, a step of the speed provokes an increment of voltage magnitude. During the ramp of the magnitude voltage, i_q current is maximum.

Afterwards this maximum affects by generating a minimum in the flux weakening current (0.5-1 min stage). In addition, positive shift in the torque affects the flux weakening by decreasing in a lower stage than before, keeping it in a constant value whilst the i_q current keeps positive in a constant value (200A). When the torque shift is negative, the i_q current decreases (-100 A) as well and the flux weakening increases in a constant stage (2-2.5 min stage).

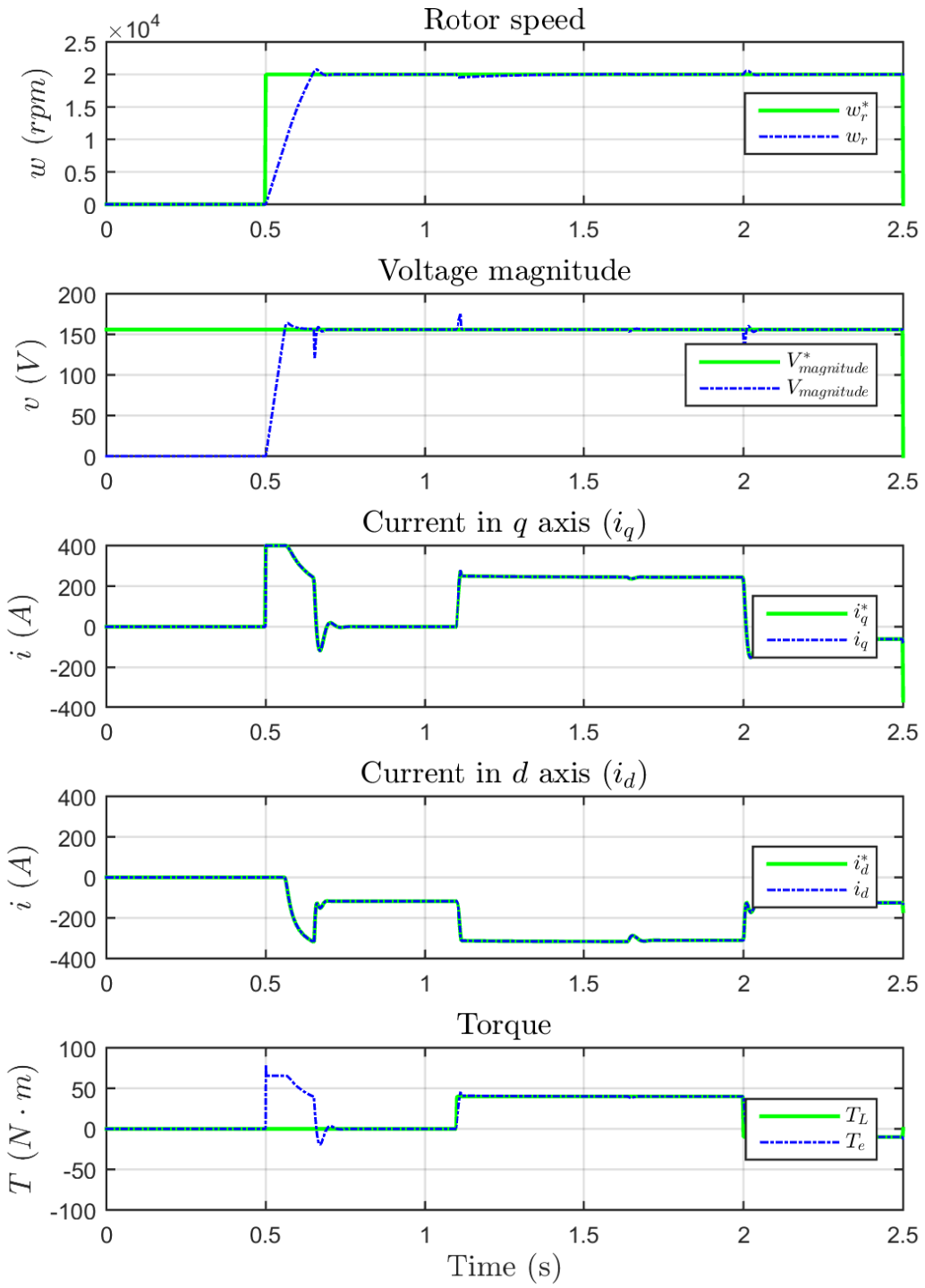

Figure 7-5: Flux weakening simulation results.

Chapter 8

Conclusions

8.0.1 Specific conclusions

The specific conclusions can be summarised as follow:

i To simplified the SPMSM control system dq coordinates have been selected. In addition, when the linear equation was obtained, the development of a PSIM simulation allows future analysis for different operating points.

ii As first assignment, the implementation of non-linear equation was selected for the entire range. For this simulation a cascade control was performed using the internal loop for controlling the current and the external loop is for the speed/torque control.

iii For the first simulation some problems arose in the control speed due to high bandwidth for the speed/torque control. This problem was solved by using an active dumping coefficient.

iv Specific design was performed in order to fulfil the aircraft standard though the final design. The result are more accurate comparing with the first model.

v Once the PIs have been designed, flux weakening is implemented to understand the behaviour of the SPSM; seeing how the i_d current affect the flux of the machine.

8.0.2 General conclusions and future prospect

The following general conclusions have been arisen from this work:

- Power Electronics can offer advantages in aerospace applications such as:
  - System efficiency improvement.
  - Aircraft systems size and weight reduction.
  - Flexibility in several parts of the aircraft system.
- There are challenges for Power Electronics in this environment that should be improved:
  - Losses.
  - Reliability.
  - Integration.

Appendix A

Simulation 1

Listing A.1: Codigo Matlab

```
clear all
close all
clc
%%
load('Master_thesis_sim1')
%% Read data
% Reducing the number of data.
Npoints=1500;

t=DataRedP(Time,Npoints);
i_q=DataRedP(i_q,Npoints);
i_q_ref=DataRedP(i_q_ref,Npoints);
i_d=DataRedP(i_d,Npoints);
i_d_ref=DataRedP(i_d_ref,Npoints);
T_e=DataRedP(T_e,Npoints);
T_L=DataRedP(T_L,Npoints);
```

```
%% Plot 'Torque vs Angle variation in MTPA $i_{dq}$' and '
    Currents vs Angle variation in MTPA $i_{dq}$'.

% Figure 1:
size_line=1.5;
size_font=12;
size_axis=9;

% Subplot 1:
x11_min=0;
x11_max=1e-3;
inc_x11=linspace(x11_min,x11_max,11);
%inc_x11=[x11_min -4 0 6 x11_max];
y11_min=-1.5;
y11_max=1.5;
inc_y11=linspace(y11_min,y11_max,7);
%inc_y11=[y11_min -4 0 6 y11_max];

figure()
plot(t,i_d_ref,'g','LineWidth',size_line);set(gca,'FontSize',
    size_axis);
hold on;
plot(t,i_d,'b-.','LineWidth',size_line-0.5);set(gca,'FontSize
    ',size_axis);
hold on;
plot(t,i_q_ref,'c','LineWidth',size_line);set(gca,'FontSize',
    size_axis);
hold on;
plot(t,i_q,'m-.','LineWidth',size_line-0.5);set(gca,'FontSize
    ',size_axis);
```

```
ylabel('$i~(A)$','interpreter','Latex','fontsize',size_font)
xlabel('Time (s)','interpreter','Latex','fontsize',size_font)
I=legend('$i_{d}^{*}$','$i_{d}$','$i_{q}^{*}$','$i_{q}$',...
    'fontsize',size_font,'Location','East');
set(I,'Interpreter','Latex');
title('Current step response','interpreter','Latex','fontsize
    ',size_font)
grid on;
axis([x11_min x11_max y11_min y11_max])
set(gca,'XTick', [inc_x11])
set(gca,'YTick', [inc_y11])

% matlab2tikz( 'Simulation_1_1.tikz','height', '\figureheight
    ',...
% 'width', '\figurewidth');
```

Appendix B

Simulation 2

Listing B.1: Codigo Matlab

```
clear all
close all
clc
%%
load('Master_thesis_sim4')
%% Read data
% Reducing the number of data.
Npoints=1500;

t=DataRedP(Time,Npoints);
w_r=DataRedP(w_r,Npoints);
w_r_ref=DataRedP(w_r_ref,Npoints);
i_q=DataRedP(i_q,Npoints);
i_q_ref=DataRedP(i_q_ref,Npoints);
i_d=DataRedP(i_d,Npoints);
i_d_ref=DataRedP(i_d_ref,Npoints);
T_e=DataRedP(T_e,Npoints);
```

```
T_L=DataRedP(T_L,Npoints);

%% Plot 'Speed step response'.

% Figure 1:
size_line=1.5;
size_font=12;
size_axis=9;

% Subplot 1:
x11_min=0;
x11_max=0.5;
inc_x11=linspace(x11_min,x11_max,6);
%inc_x11=[x11_min -4 0 6 x11_max];
y11_min=0;
y11_max=2000;
inc_y11=linspace(y11_min,y11_max,5);
%inc_y11=[y11_min -4 0 6 y11_max];


figure()
plot(t,w_r_rpm_ref,'g','LineWidth',size_line);set(gca,'
    FontSize',size_axis);
hold on;
plot(t,w_r_rpm,'b-.','LineWidth',size_line-0.5);set(gca,'
    FontSize',size_axis);

ylabel('$w^(rpm)$','interpreter','Latex','fontsize',size_font
    )
xlabel('Time_(s)','interpreter','Latex','fontsize',size_font)
```

```
I=legend('$w_{r}^{*}$','$w_{r}$',...
    'fontsize',size_font,'Location','East');
title('Speed step response','interpreter','Latex','fontsize',
   size_font)
set(I,'Interpreter','Latex');
grid on;
axis([x11_min x11_max y11_min y11_max])
set(gca,'XTick', [inc_x11])
set(gca,'YTick', [inc_y11])

% matlab2tikz( 'Simulation_2_1.tikz','height', '\figureheight
   ',...
% 'width', '\figurewidth');
%% Plot 'Rotor speed' and 'Torque'.

% Figure 2:
size_line=1.5;
size_font=12;
size_axis=9;

% Subplot 1:
x21_min=0;
x21_max=3;
inc_x21=linspace(x21_min,x21_max,7);
%inc_x21=[x21_min -4 0 6 x21_max];
y21_min=0;
y21_max=3000;
inc_y21=linspace(y21_min,y21_max,5);
%inc_y21=[y21_min -4 0 6 y21_max];
```

```
% Subplot 2:
x22_min=0;
x22_max=3;
inc_x22=linspace(x22_min,x22_max,7);
%inc_x22=[x22_min -4 0 6 x22_max];
y22_min=-100;
y22_max=150;
inc_y22=linspace(y22_min,y22_max,6);
%inc_y22=[y22_min -4 0 6 y22_max];
%


figure()
subplot(211)
plot(t,w_r_rpm_ref,'g','LineWidth',size_line);set(gca,'
    FontSize',size_axis);
hold on;
plot(t,w_r_rpm,'b-.','LineWidth',size_line-0.5);set(gca,'
    FontSize',size_axis);

ylabel('$w~(rpm)$','interpreter','Latex','fontsize',size_font
    )
% xlabel('Time (s)','interpreter','Latex','fontsize',
    size_font)
I=legend('$w_{r}^{*}$','$w_{r}$',...
     'fontsize',size_font,'Location','East');
title('Rotor_speed','interpreter','Latex','fontsize',
    size_font)
set(I,'Interpreter','Latex');
grid on;
```

```
axis([x21_min x21_max y21_min y21_max])
set(gca,'XTick', [inc_x21])
set(gca,'YTick', [inc_y21])

subplot(212)
plot(t,T_L,'g','LineWidth',size_line);set(gca,'FontSize',
    size_axis);
hold on;
plot(t,T_e,'b-.','LineWidth',size_line -0.5);set(gca,'FontSize
    ',size_axis);

ylabel('$T~(N\cdot m)$','interpreter','Latex','fontsize',
    size_font)
xlabel('Time (s)','interpreter','Latex','fontsize',size_font)
I=legend('$T_{L}$','$T_{e}$',...
     'fontsize',size_font,'Location','East');
title('Torque','interpreter','Latex','fontsize',size_font)
set(I,'Interpreter','Latex');
grid on;
axis([x22_min x22_max y22_min y22_max])
set(gca,'XTick', [inc_x22])
set(gca,'YTick', [inc_y22])

% matlab2tikz( 'Simulation_2_2.tikz','height', '\figureheight
    ',...
% 'width', '\figurewidth');
%% Plot 'Rotor speed', 'Currents in dq axis' and 'Torque'.

% Figure 3:
size_line=1.5;
```

```
size_font=12;
size_axis=9;

% Subplot 1:
x31_min=0;
x31_max=3;
inc_x31=linspace(x31_min,x31_max,7);
%inc_x31=[x31_min -4 0 6 x31_max];
y31_min=0;
y31_max=3000;
inc_y31=linspace(y31_min,y31_max,5);
%inc_y31=[y31_min -4 0 6 y31_max];

% Subplot 2:
x32_min=0;
x32_max=3;
inc_x32=linspace(x32_min,x32_max,7);
%inc_x32=[x2_min -4 0 6 x32_max];
y32_min=-600;
y32_max=800;
inc_y32=linspace(y32_min,y32_max,8);
%inc_y32=[y32_min -4 0 6 y32_max];
%

% Subplot 3:
x33_min=0;
x33_max=3;
inc_x33=linspace(x33_min,x33_max,7);
%inc_x33=[x33_min -4 0 6 x33_max];
y33_min=-20;
```

```
y33_max=10;
inc_y33=linspace(y33_min,y33_max,7);
%inc_y33=[y33_min -4 0 6 y33_max];
%

% Subplot 4:
x34_min=0;
x34_max=3;
inc_x34=linspace(x34_min,x34_max,7);
%inc_x34=[x34_min -4 0 6 x34_max];
y34_min=-100;
y34_max=150;
inc_y34=linspace(y34_min,y34_max,6);
%inc_y34=[y34_min -4 0 6 y34_max];
%


figure()
subplot(411)
plot(t,w_r_rpm_ref,'g','LineWidth',size_line);set(gca,'
    FontSize',size_axis);
hold on;
plot(t,w_r_rpm,'b-.','LineWidth',size_line-0.5);set(gca,'
    FontSize',size_axis);

ylabel('$w~(rpm)$','interpreter','Latex','fontsize',size_font
    )
% xlabel('Time (s)','interpreter','Latex','fontsize',
    size_font)
I=legend('$w_{r}^{*}$','$w_{r}$',...
```

```
    'fontsize',size_font,'Location','East');
title('Rotor speed','interpreter','Latex','fontsize',
    size_font)
set(I,'Interpreter','Latex');
grid on;
axis([x31_min x31_max y31_min y31_max])
set(gca,'XTick', [inc_x31])
set(gca,'YTick', [inc_y31])

subplot(412)
plot(t,i_q_ref,'g','LineWidth',size_line);set(gca,'FontSize',
    size_axis);
hold on;
plot(t,i_q,'b-.','LineWidth',size_line-0.5);set(gca,'FontSize
    ',size_axis);

ylabel('$i^(A)$','interpreter','Latex','fontsize',size_font)
% xlabel('Time (s)','interpreter','Latex','fontsize',
    size_font)
I=legend('$i_{q}^{*}$','$i_{q}$',...
    'fontsize',size_font,'Location','East');
title('Current in $q$ axis ($i_{q}$)','interpreter','Latex','
    fontsize',size_font)
set(I,'Interpreter','Latex');
grid on;
axis([x32_min x32_max y32_min y32_max])
set(gca,'XTick', [inc_x32])
set(gca,'YTick', [inc_y32])

subplot(413)
```

```
plot(t,i_d_ref,'g','LineWidth',size_line);set(gca,'FontSize',
    size_axis);
hold on;
plot(t,i_d,'b-.','LineWidth',size_line-0.5);set(gca,'FontSize
    ',size_axis);

ylabel('$i~(A)$','interpreter','Latex','fontsize',size_font)
% xlabel('Time (s)','interpreter','Latex','fontsize',
    size_font)
I=legend('$i_{d}^{*}$','$i_{d}$',...
     'fontsize',size_font,'Location','East');
title('Current in $d$ axis ($i_{d}$)','interpreter','Latex','
    fontsize',size_font)
set(I,'Interpreter','Latex');
grid on;
axis([x33_min x33_max y33_min y33_max])
set(gca,'XTick', [inc_x33])
set(gca,'YTick', [inc_y33])

subplot(414)
plot(t,T_L,'g','LineWidth',size_line);set(gca,'FontSize',
    size_axis);
hold on;
plot(t,T_e,'b-.','LineWidth',size_line-0.5);set(gca,'FontSize
    ',size_axis);

ylabel('$T~(N\cdot m)$','interpreter','Latex','fontsize',
    size_font)
xlabel('Time (s)','interpreter','Latex','fontsize',size_font)
I=legend('$T_{L}$','$T_{e}$',...
```

```
    'fontsize',size_font,'Location','East');
title('Torque','interpreter','Latex','fontsize',size_font)
set(I,'Interpreter','Latex');
grid on;
axis([x34_min x34_max y34_min y34_max])
set(gca,'XTick', [inc_x34])
set(gca,'YTick', [inc_y34])

% matlab2tikz( 'Simulation_2_3.tikz','height', '\figureheight
    ',...
% 'width', '\figurewidth');
```

Appendix C

Simulation 3

Listing C.1: Codigo Matlab

```
clear all
close all
clc
%%
load('Master_thesis_sim3')
%% Read data
% Reducing the number of data.
Npoints=1500;

t=DataRedP(Time,Npoints);
w_r=DataRedP(w_r,Npoints);
w_r_ref=DataRedP(w_r_ref,Npoints);
i_q=DataRedP(i_q,Npoints);
i_q_ref=DataRedP(i_q_ref,Npoints);
i_d=DataRedP(i_d,Npoints);
i_d_ref=DataRedP(i_d_ref,Npoints);
T_e=DataRedP(T_e,Npoints);
```

```
T_L=DataRedP(T_L,Npoints);

%% Plot 'Speed step response'.

% Figure 1:
size_line=1.5;
size_font=12;
size_axis=9;

% Subplot 1:
x11_min=0;
x11_max=0.5;
inc_x11=linspace(x11_min,x11_max,6);
%inc_x11=[x11_min -4 0 6 x11_max];
y11_min=0;
y11_max=20;
inc_y11=linspace(y11_min,y11_max,5);
%inc_y11=[y11_min -4 0 6 y11_max];


figure()
plot(t,w_r_ref,'g','LineWidth',size_line);set(gca,'FontSize',
    size_axis);
hold on;
plot(t,w_r,'b-.','LineWidth',size_line-0.5);set(gca,'FontSize
    ',size_axis);

ylabel('$w^(rpm)$','interpreter','Latex','fontsize',size_font
    )
xlabel('Time_(s)','interpreter','Latex','fontsize',size_font)
```

```
I=legend('$w_{r}^{*}$','$w_{r}$',...
    'fontsize',size_font,'Location','East');
title('Speed step response','interpreter','Latex','fontsize',
   size_font)
set(I,'Interpreter','Latex');
grid on;
axis([x11_min x11_max y11_min y11_max])
set(gca,'XTick', [inc_x11])
set(gca,'YTick', [inc_y11])

% matlab2tikz( 'Simulation_3_1.tikz','height', '\figureheight
   ',...
% 'width', '\figurewidth');
%% Plot 'Rotor speed', 'Currents in dq axis' and 'Torque'.

% Figure 2:
size_line=1.5;
size_font=12;
size_axis=9;

% Subplot 1:
x21_min=0;
x21_max=3;
inc_x21=linspace(x21_min,x21_max,7);
%inc_x21=[x21_min -4 0 6 x21_max];
y21_min=0;
y21_max=40;
inc_y21=linspace(y21_min,y21_max,5);
%inc_y21=[y21_min -4 0 6 y21_max];
```

```
% Subplot 2:
x22_min=0;
x22_max=3;
inc_x22=linspace(x22_min,x22_max,7);
%inc_x22=[x22_min -4 0 6 x22_max];
y22_min=-500;
y22_max=1000;
inc_y22=linspace(y22_min,y22_max,7);
%inc_y22=[y22_min -4 0 6 y22_max];
%

% Subplot 3:
x23_min=0;
x23_max=3;
inc_x23=linspace(x23_min,x23_max,7);
%inc_x23=[x23_min -4 0 6 x23_max];
y23_min=-20;
y23_max=10;
inc_y23=linspace(y23_min,y23_max,7);
%inc_y23=[y23_min -4 0 6 y23_max];
%

% Subplot 4:
x24_min=0;
x24_max=3;
inc_x24=linspace(x24_min,x24_max,7);
%inc_x24=[x24_min -4 0 6 x24_max];
y24_min=-100;
y24_max=200;
inc_y24=linspace(y24_min,y24_max,7);
```

```
%inc_y24=[y24_min -4 0 6 y24_max];
%


figure()
subplot(411)
plot(t,w_r_ref,'g','LineWidth',size_line);set(gca,'FontSize',
    size_axis);
hold on;
plot(t,w_r,'b-.','LineWidth',size_line -0.5);set(gca,'FontSize
    ',size_axis);

ylabel('$w~(rpm)$','interpreter','Latex','fontsize',size_font
    )
% xlabel('Time (s)','interpreter','Latex','fontsize',
    size_font)
I=legend('$w_{r}^{*}$','$w_{r}$',...
     'fontsize',size_font,'Location','East');
title('Rotor speed','interpreter','Latex','fontsize',
    size_font)
set(I,'Interpreter','Latex');
grid on;
axis([x21_min x21_max y21_min y21_max])
set(gca,'XTick', [inc_x21])
set(gca,'YTick', [inc_y21])

subplot(412)
plot(t,i_q_ref,'g','LineWidth',size_line);set(gca,'FontSize',
    size_axis);
hold on;
```

```
plot(t,i_q,'b-.','LineWidth',size_line-0.5);set(gca,'FontSize
    ',size_axis);

ylabel('$i~(A)$','interpreter','Latex','fontsize',size_font)
% xlabel('Time (s)','interpreter','Latex','fontsize',
    size_font)
I=legend('$i_{q}^{*}$','$i_{q}$',...
     'fontsize',size_font,'Location','East');
title('Current in $q$ axis ($i_{q}$)','interpreter','Latex','
    fontsize',size_font)
set(I,'Interpreter','Latex');
grid on;
axis([x22_min x22_max y22_min y22_max])
set(gca,'XTick', [inc_x22])
set(gca,'YTick', [inc_y22])

subplot(413)
plot(t,i_d_ref,'g','LineWidth',size_line);set(gca,'FontSize',
    size_axis);
hold on;
plot(t,i_d,'b-.','LineWidth',size_line-0.5);set(gca,'FontSize
    ',size_axis);

ylabel('$i~(A)$','interpreter','Latex','fontsize',size_font)
% xlabel('Time (s)','interpreter','Latex','fontsize',
    size_font)
I=legend('$i_{d}^{*}$','$i_{d}$',...
     'fontsize',size_font,'Location','East');
title('Current in $d$ axis ($i_{d}$)','interpreter','Latex','
    fontsize',size_font)
```

```
set(I,'Interpreter','Latex');
grid on;
axis([x23_min x23_max y23_min y23_max])
set(gca,'XTick', [inc_x23])
set(gca,'YTick', [inc_y23])

subplot(414)
plot(t,T_L,'g','LineWidth',size_line);set(gca,'FontSize',
    size_axis);
hold on;
plot(t,T_e,'b-.','LineWidth',size_line -0.5);set(gca,'FontSize
    ',size_axis);

ylabel('$T~(N\cdot m)$','interpreter','Latex','fontsize',
    size_font)
xlabel('Time (s)','interpreter','Latex','fontsize',size_font)
I=legend('$T_{L}$','$T_{e}$',...
     'fontsize',size_font,'Location','East');
title('Torque','interpreter','Latex','fontsize',size_font)
set(I,'Interpreter','Latex');
grid on;
axis([x24_min x24_max y24_min y24_max])
set(gca,'XTick', [inc_x24])
set(gca,'YTick', [inc_y24])

% matlab2tikz( 'Simulation_3_2.tikz','height', '\figureheight
    ',...
% 'width', '\figurewidth');
```

Appendix D

Transfer function with i_q not limited

Listing D.1: Codigo Matlab

```
clear all
close all
clc
%% Starter mode with iq_ref not limited:
s=tf('s');

% Variables: i_dq/i_dq*
BWi_Hz=1000;            % Bandwidth (Hz)
Xii=sqrt(2)/2;          %
w_ni=2*pi*BWi_Hz;       %
L=99e-6;                % Stator inductance in rotating frame (H)
    Lq=Ld=L
R=1.058e-3;         % Stator resistance, Rs (Ohm) R=Rs
% Transfer function: i_dq/i_dq*
G_idq_idq_ref=((2*Xii*w_ni*L-R)*s+w_ni^2*L)/(L*(s^2+2*Xii*
```

```
    w_ni*s+w_ni^2))
% sisotool(G_idq_idq_ref)

% Variables: d|V|/i_d*
v_d0=-1.2428925e-001;
v_q0=1.5588457e+002;
Vmag0=1.5588457e+002;
w_e0=6.2831853e+003;
% Transfer function: d|V|/i_d*
G_V_id_ref=G_idq_idq_ref*[(v_d0/Vmag0)*(R+L*s)+(v_q0/Vmag0)*(
    L*w_e0)]
% sisotool(G_V_id_ref)

%%
load('iq_not_limited')
%%
%% Read data
% Reducing the number of data.
[step_response,t_step]=step(G_V_id_ref);

Npoints=length(t_step);

t=DataRedP(Time,Npoints);
Time=DataRedP(Time,Npoints);
i_d=DataRedP(i_d,Npoints);
i_d(104)=i_d(103);

[step_response,t_step]=step(G_V_id_ref);
plot(t_step,step_response)
hold on
```

```
plot(t_step,i_d+1.1747676e+002)

ylabel('$i~(A)$','interpreter','Latex')
xlabel('Time (s)','interpreter','Latex')
I=legend('$i_{d_{FUNCTION}}^*$','$i_{d_{SYSTEM}}^*$',...
    'Location','East');
set(I,'Interpreter','Latex');
title('Step response $\frac{V}{i_d}$: FUNCTION vs SYSTEM','
    interpreter','Latex')
grid on;
```

Bibliography

[1] S. Bozhko, S. S. Yeoh, F. Gao, and C. Hill. Aircraft starter-generator system based on permanent-magnet machine fed by active front-end rectifier. In *Industrial Electronics Society, IECON 2014 - 40th Annual Conference of the IEEE*, pages 2958–2964, Oct 2014.

[2] Gene F. Franklin, J. David Powell, and Abbas Emami-Naeini. *Feedback Control of Dynamic Systems*. Prentice Hall, fifth edition, 2005.

[3] F. Gao, S. Bozhko, Y. Seang Shen, and G. Asher. Control design for pmm starter-generator operated in flux-weakening mode. In *Power Engineering Conference (UPEC), 2013 48th International Universities'*, pages 1–6, Sept 2013.

[4] D. W. Novotny and T. A. Lipo. *Vector Control and Dynamics of AC Drives*. OXFORD SCIENCE PUBLICATIONS, 1996.

[5] Y. Seang Shen, L. Xia, S. Bozhko, and G. Asher. Stability analysis of aircraft electrical power system with active front rectifier system in generation channel. In *Power Engineering Conference (UPEC), 2013 48th International Universities'*, pages 1–6, Sept 2013.

[6] S. S. Yeoh, F. Gao, S. Bozhko, and G. Asher. Control design for pmm-based starter generator system for more electric aircraft. In *Power Electronics and Applications (EPE'14-ECCE Europe), 2014 16th European Conference on*, pages 1–10, Aug 2014.